COMMUNICATIONS

Magnetic Resonance in Medicine 59:441–446 (2008)

B_1^+ Compensation in 3T Cardiac Imaging Using Short 2DRF Pulses

Kyunghyun Sung* and Krishna S. Nayak

The purpose of this study was to determine if tailored 2DRF pulses could be used to compensate for in-plane variations of the transmitted RF field at 3T. Excitation pulse profiles were designed to approximate the reciprocal of the measured RF transmit variation where the variation over the left ventricle was approximated as unidirectional. A simple 2DRF pulse design utilizing three subpulses was used, such that profiles could be quickly and easily adapted to different regions of interest. Results are presented from phantom and in vivo cardiac imaging. Compared with conventional slice-selective excitation, the average flip angle variation over the left ventricle (measured as the standard deviation divided by the mean flip angle) was reduced with $P < 0.001$ and the average reduction was 41% in cardiac studies at 3T. Magn Reson Med 59:441–446, 2008.

Key words: RF non-uniformity; B_1 compensation; 2D RF pulse design; high-field imaging

The spatial distribution of the radio frequency (RF) field used for excitation and reception has an important influence on image quality in magnetic resonance imaging (MRI). Inhomogeneous RF transmission (B_1^+) produces nonuniform flip angles, causing spatially dependent tissue contrast and signal intensity. This is a critical source of error when quantifying NMR parameters from image data. B_1^+ nonuniformity is influenced by several factors including the distance from the RF transmit coil, conductivity, tissue dielectric constant, and factors related to the body size and RF wavelength. Methods for reducing B_1^+ inhomogeneity are highly desirable in high field imaging (1–4) and imaging with surface coil transmission (5). In high-field cardiac imaging ($\geq$ 3T), B_1^+ inhomogeneity on the order of 30–50% across the imaging volume has been predicted and observed (1, 6–9).

One method to address B_1^+ inhomogeneity is single transmit channel RF shimming using 2D or 3D tailored RF excitation pulses. Homogeneous tissue excitation can be achieved by tailoring the excitation with a spatial profile that is approximately equal to the reciprocal of the B_1^+ variation. The physical B_1^+ inhomogeneity is still present, but uniform excitation can be achieved. Several methods using the tailored RF pulses have been proposed for neurologic applications (10,11). Diechmann et al. (10) described an RF excitation pulse that performs rapid 2D compensation and was effective for structural 3D brain imaging. Small tip-angle 3D tailored RF pulses designed by Saekho et al. (11) included slice selection and were also promising in neuro imaging. Both pulse designs, however, are limited to a small family of variation patterns and not fully based on B_1^+ measurement.

In 3T cardiac imaging, the patterns of B_1^+ variation across the heart are different from the typical patterns in brain imaging. More severe and diverse patterns of variation are expected because the chest is of comparable dimension to the RF wavelength at 3T (1,6–9). Tailored RF pulse designs based on actual measurements are needed for robust B_1^+ compensation. Until recently, this approach has been limited by (a) the lack of time-efficient and volumetric methods for B_1^+ mapping, and (b) long duration of appropriate tailored RF pulses. The saturated double angle method (SDAM) (8) was recently demonstrated as a rapid and appropriate method for B_1^+ mapping in the chest at 3T (9). Performed in a single breath-hold, this method can provide accurate and repeatable in vivo B_1^+ measurement covering the whole heart in a single breath-hold (9). The most recent study involving 10 subjects and two scanners found the pattern of flip angle variation to be largely unidirectional across the heart when using a single-channel conventional body-coil for RF transmission (9). This suggests the possibility of a one-dimensional B_1^+ compensation scheme using short 2DRF pulses, which is simpler and potentially more robust than 3D tailored RF schemes.

In this manuscript, we introduce a short tailored 2DRF pulse for compensating for B_1^+ nonuniformity in single transmit channel slice-selective cardiac imaging. The pulse utilizes a fly-back echo-planar trajectory in excitation k-space, enabling a measurement-based adjustment of excitation profiles to compensate in-plane B_1^+ variations. The unidirectional B_1^+ compensation method was demonstrated and evaluated in phantoms, and in vivo cardiac imaging at 3T.

MATERIALS AND METHODS

2DRF Pulse

For small-tip excitation, 2DRF pulses can be designed and analyzed with the excitation k-space framework developed by Pauly et al. (12). Ignoring relaxation and off-resonance, the transverse magnetization M_{xy} is proportional to the Fourier Transform (FT) of the product of a spatial frequency weighting function $W(k)$ and a spatial frequency sampling function $S(k)$ (12,13).

Magnetic Resonance Engineering Laboratory, Ming Hsieh Department of Electrical Engineering, University of Southern California, Los Angeles, California

Grant sponsor: American Heart Association; Grant number: 0435249N

Grant sponsors: Korea Science and Engineering Foundation, James H. Zumberge Foundation, GE Healthcare

*Correspondence to: Kyunghyun Sung, Department of Electrical Engineering, 3740 McClintock Ave, EEB 412, University of Southern California, Los Angeles, CA 90089-2564. E-mail: kyunghsu@sipi.usc.edu

Received 05 April 2007; revised 17 July 2007; accepted 16 September 2007.

DOI 10.1002/mrm.21443

Published online 24 January 2008 in Wiley InterScience (www.interscience.wiley.com).

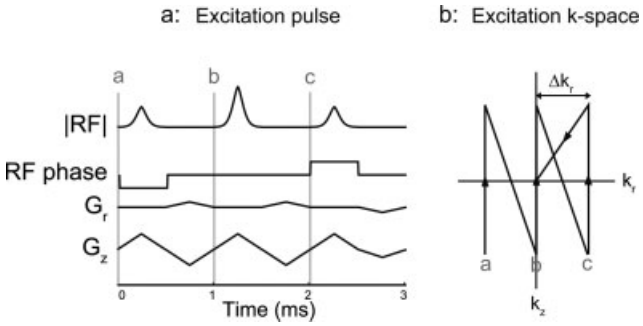

FIG. 1. Proposed 2DRF excitation for B_1^+ compensation: (**a**) excitation pulse and (**b**) excitation k-space trajectory. The subpulse duration is 0.5 msec, and overall duration is 3 msec including all gradients. A fly-back echo-planar design is used where RF is only transmitted during positive gradient lobes of G_z. Note that points a, b, and c indicate the same point on time on both (a) and (b).

The 2D echo-planar excitation k-space trajectory is suitable in this work because the design considerations for slice selection and B_1^+ compensation are independent and separable (14,15). The pulse design involves two stages: the design of subpulses (fast direction, k_z) and the design of subpulse weightings (slow direction, k_r). The subpulse design is based on the desired slice profile, and the r-axis can be any in-plane radial axis, as determined by the 1D approximation (9).

For the r-axis, the excitation pulse profile $\widehat{f}(r)$ can be written as

$$\widehat{f}(r) \propto FT(W(k_r) \cdot S(k_r)). \quad [1]$$

Assuming the sampling density Δk_r is uniform and the number of subpulses is odd $(2N+1)$, $W(k_r) \cdot S(k_r)$ may be expressed as

$$W(k_r) \cdot S(k_r) = \sum_{n=-N}^{N} A_n \cdot \delta(k_r - n\Delta k_r) \cdot e^{i\theta_n k_r}, \quad [2]$$

where $\delta(k_r)$ is the Kronecker delta function. $\widehat{f}(r)$ is the FT of the series of delta functions with subpulse weighting A_n and phase θ_n. Standard methods for finite impulse response (FIR) filter design provide an excellent way to obtain an appropriate $\widehat{f}(r)$.

Figure 1 shows the proposed RF pulse and the corresponding excitation k-space trajectory. G_r represents a combination of the logical G_x and G_y gradients. The RF subpulse duration is 0.5 msec while the overall pulse duration including refocusing gradient lobe is 3 msec, sufficiently fast for cardiac imaging.

The individual subpulse shape was designed using the Shinnar–LeRoux (SLR) algorithm (16). Subpulse duration was minimized by taking full advantage of the gradients (40 mT/m amplitude and 150 T/m/sec slew rate) and RF capabilities (peak $B_1 = 16\mu T$). A time-bandwidth product (TB) of 2 was used for slice selection (5 mm slice thickness). The variable-rate selective excitation (VERSE) technique was applied to compensate for the fact that RF is transmitted during gradient ramps (17).

For the in-plane flip angle variation, we set the number of subpulses as three to make the total pulse duration as short as possible and used a 1-2-1 binomial weighting $(A_{-1} = 1, A_0 = 2, A_1 = 1)$ in all studies. We also used a phase increment $\theta(\theta_{-1} = -\theta, \theta_0 = 0, \theta_1 = \theta)$. With these conditions, $\widehat{f}(r)$ becomes simply a raised cosine:

$$\widehat{f}(r) = \frac{\alpha_{\max}}{2}(1 + \cos(\Delta k_r \cdot r + \theta)). \quad [3]$$

where $\alpha_{\max}$ is the peak flip angle value in $\widehat{f}(r)$.

Tailored 2DRF Pulse Design Based on Measurement

Figure 2 illustrates the tailored 2DRF pulse design procedure based on B_1^+ measurement. The flip angle variation $\alpha_{\text{measured}}(x, y)$ is first measured using SDAM (8,9) and can be expressed as

$$\alpha_{\text{measured}}(x, y) = \alpha_{\text{nom}} \cdot b_1(x, y) \quad [4]$$

where α_{nom} is the nominal flip angle entered in the scanner and $b_1(x, y)$ is the spatially varying relative RF amplitude.

Circular regions of interest (ROIs) covering left ventricular myocardium and blood pool are then manually selected based on magnitude images. A one-dimensional approximation $\alpha_{\text{measured}}(r)$ is computed by minimizing mean square error (MMSE) along the primary in-plane axis (dotted line in Fig. 2). MMSE 1D approximations are computed at all angles with a 1° increment, and the primary in-plane

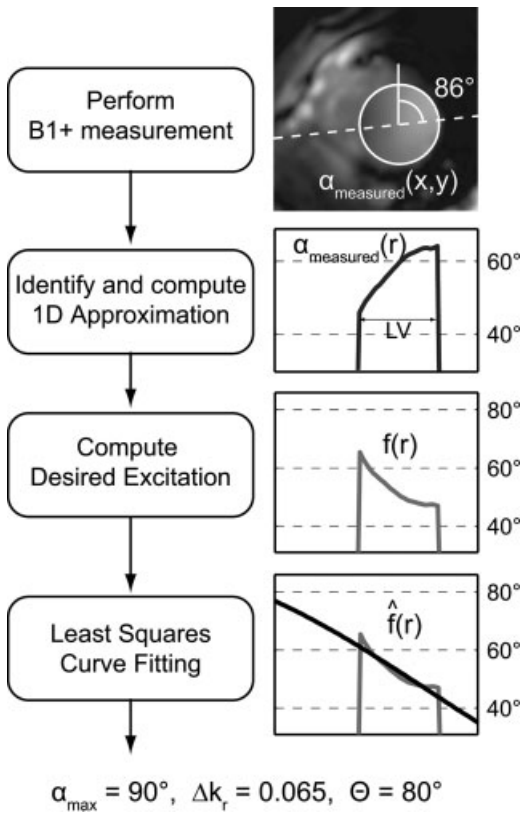

FIG. 2. Measurement-based tailored 2DRF pulse design procedure. Data from one slice in a cardiac study are shown for illustration. In this example, the computed control parameters were: the primary in-plane axis = 86°, $\alpha_{\max} = 90°$, $\Delta k_r = 0.065$, and $\theta = 80°$.

axis, r, is defined such that it minimizes the approximation error.

The desired excitation pulse profile $f(r)$ is then simply defined as the reciprocal of $\alpha_{\text{measured}}(r)$ to cancel out the RF transmit variation.

$$f(r) = \alpha_{\text{target}}/b_1(r) \quad [5]$$

where α_{target} is the intended flip angle after B_1^+ compensation.

To produce a practical approximation, $\widehat{f}(r)$, and identify design parameters: $\alpha_{\max}$, Δk_r, and θ, the nonlinear curve-fitting problem is solved in the least-squares sense (Optimization Toolbox, MATLAB 7.0), minimizing:

$$\min_{\alpha_{\max},\Delta k_r,\theta} \frac{1}{2} \sum_{r_n \in \text{ROI}} (f(r_n) - \widehat{f}(r_n))^2. \quad [6]$$

Note that $\alpha_{\max}$ had a upper bound of 90° and θ was allowed to range from $-\pi/2$ to $\pi/2$. The r-axis, $\alpha_{\max}$, Δk_r, and θ were calculated separately for each slice in multislice studies.

Experimental Methods

Experiments were performed on two GE Signa 3.0 T EXCITE systems (General Electric Healthcare, Waukesha, WI) each with gradients capable of 40 mT/m amplitude and 150 T/m/sec slew rate, and a receiver supporting 4 μsec sampling (±125 kHz). The transmit gain was calibrated using a standard pre-scan and the localized center frequency was adjusted over a 3D region of interest.

To evaluate the proposed approach, we used two sets of excitation pulses: a slice-selective RF pulse and the proposed 2DRF pulse. The slice-selective RF pulse was made by removing the G_r gradient from the 2DRF pulse and therefore had the same pulse duration. The 2DRF pulse has an amplitude 1.8 times higher than that of the reference slice-selective pulse and a 3.24 times increase in specific absorption rate (SAR). Two magnitude base images (I_{α_1} and $I_{2\alpha_1}$) were acquired (18) to measure the flip angle variation. Because $I_{2\alpha_1}$ has a nominal flip angle of $2\alpha_1$, the proposed RF pulse needed to be able to accommodate a maximum flip angle of 180° and therefore was redesigned with twice the pulse duration (6 msec). In each dataset, the mean and standard deviation (SD) of flip angle over the ROI was measured. The value of the SD/mean (%) was used as metric, independent of the transmit gain, to quantify the amount of the flip angle variation. Statistical comparison of the SD/mean was performed using ANOVA and a P-value of less than 0.05 was considered statistically significant.

Phantom Experiments

In the phantom study, a single-channel birdcage transmit/receive head coil was used. A 28 cm diameter ball phantom was positioned halfway out at the end of the coil to artificially produce B_1^+ non-uniformity. Imaging was performed with a 2DFT gradient-echo (GRE) acquisition, 30 cm FOV, 256 × 256 matrix size, and 5 mm slice thickness. During reconstruction, a Gaussian filter was applied to smooth the base images.

In Vivo Experiments

In-vivo testing was performed in five healthy volunteers (4 males and 1 female, weights 55–88 kg). The Institutional Review Board of the University of Southern California approved the imaging protocols. Each subject was screened for magnetic resonance imaging risk factors and provided informed consent in accordance with institutional policy.

The body coil was used for RF transmission and an 8-channel phased array cardiac coil was used for signal reception. Scan plane localization was performed using the GE I-drive real-time system. In each volunteer, 4–6 parallel short axis slices were prescribed spanning the left ventricle (LV) from base to apex. The basal slice was denoted as no. 1 and the apical slice was denoted as no. 6. A multislice spiral imaging acquisition was used within a single breath-hold of 16 R-R intervals (FOV = 30 cm). Acquisitions were cardiac gated using either plethysmograph (4 subjects) or ECG signals (1 subject), with imaging occurring in mid-diastole. During reconstruction, a Hamming window was applied to k-space data to increase the base image SNR while reducing the in-plane spatial resolution to 5 mm.

RESULTS

Figure 3 contains a comparison between measured and simulated excitation profiles with and without off-resonance (−440 Hz). The excitation pulse profile $\widehat{f}(r)$ was measured using a ball phantom with a spin-echo pulse sequence and computed with numerical Bloch simulation. The slice thickness (full-width at half maximum) of measured profiles was 22% thicker and, as expected, off-resonance caused a shift along the r-axis.

Figure 4 illustrates measured changes in the excitation pulse profile when modifying the three control parameters. Any axis of variation can be formed by using both the logical G_x and G_y gradients (Fig. 4a). Δk_r changes the period of

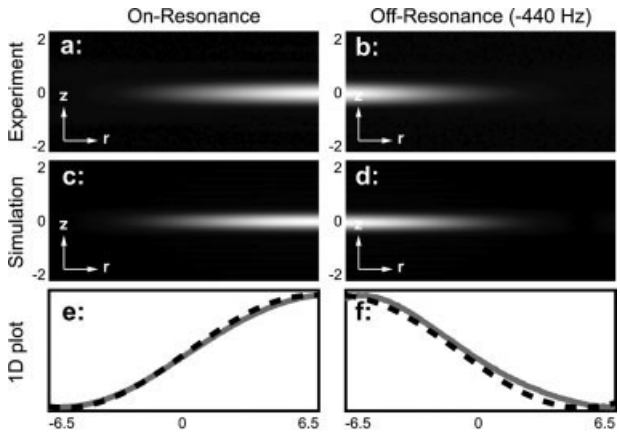

FIG. 3. Measured (**a** and **b**) and simulated (**c** and **d**) excitation profiles of the proposed 2DRF pulse. The cross-section plots (**e** and **f**) along the r-direction show an excellent agreement between experiment (solid line) and simulation (dotted line). The measured slice thickness was 22% larger than simulation. As expected, off-resonance results in a profile shift along the r-axis.

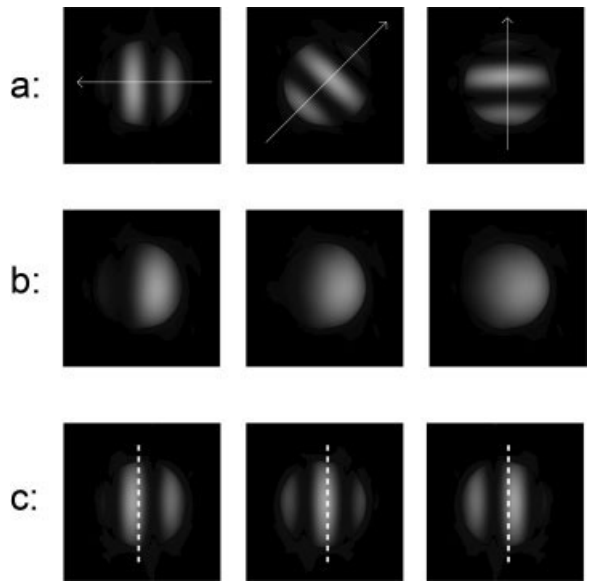

FIG. 4. Illustration of 2DRF excitation profile control using the design parameters: (**a**) $\vec{r}$, the radial axis of variation, (**b**) Δk_r, the frequency of variation, and (**c**) θ, profile shifting. After the primary in-plane axis is determined from the measured B_1^+ profile, the parameters (Δk_r, θ, and α_{max}) are chosen by nonlinear least squares estimation. Note that higher Δk_r value was used in (a) and (c), containing multiple null points.

$\widehat{f}(r)$ (Fig. 4b). The phase increment θ for each RF subpulse shifts $\widehat{f}(r)$ along the r-axis (Fig. 4c).

Figure 5 contains the results of 2DRF B_1^+ compensation in a phantom. An artificial flip angle variation, from left to right, was generated by placing the ball phantom halfway out at the end of the transmit-receive head coil. A circular ROI was manually selected to cover a region with B_1^+ variation. Both α_{nom} and α_{target} were set to 60°. The flip angle experienced within the ROI was 53.9° ± 5.6° (mean ± SD) using the slice-selective RF pulse and was 59.3°±2.9° using the proposed 2DRF pulse. The value of SD/mean was reduced from 10.4% to 4.9%. The expected SD/mean predicted by simulation, and considered as a lower bound of this methodology, was 3.8% (60.7° ± 2.3°).

Figure 6 contains one of the most successful results of 2DRF B_1^+ compensation in cardiac imaging at 3T. Magnitude images provide anatomical landmarks, and the circular ROIs covered the LV in all short-axis scan planes. We set α_{nom} to 60° and α_{target} to 50°. In this mid-short-axis slice, the primary in-plane axis was 89°. The flip angle experienced within the ROI was 58° ± 4.1° (mean ± SD) using the slice-selective RF pulse and was 51° ± 0.9° using the proposed 2DRF pulse. The value of SD/mean was reduced from 7.0% to 1.8%. Considering all five slices in this subject, the flip angle SD/mean was significantly reduced with $P = 0.0126$ (4.4% - 8.4% using conventional excitation and 1.8% - 5.5% using the proposed 2DRF pulse).

Figure 7 illustrates the improvement in all six slices in another subject at 3T. The mean and SD flip angle plots (Fig. 7a,b) in all six slices show the improved flip angle uniformity and accuracy of the mean flip angle over the LV. The vertical axis indicates the percentage of the intended flip angle ($\alpha_{nom} = 60°$ for slice-selective RF and $\alpha_{target} = 50°$ for 2DRF). Figure 7c shows a bar graph containing the values of SD/mean for the slice-selective RF pulse and the proposed 2DRF pulse (expected and measured). 9.0%–10.8% flip angle variation was reduced to 5.0%–7.1%. Considering all slices in all five subjects, the SD/mean was significantly smaller with $P < 0.001$ and the average reduction was 41%. Note that the measured values (white bars) are similar to the expected values in simulation (gray bars) except in the basal slice (slice no. 1). We suspect that off-resonance in the basal slice may have contributed to this deviation.

DISCUSSION

We have demonstrated that short tailored 2DRF pulses are a practical option for B_1^+ inhomogeneity compensation in slice-selective cardiac imaging at 3T. 2DRF pulses were designed to excite spins with a pulse profile that is approximately the reciprocal of the measured variation. However, when the transmitted B_1^+ is close to zero due to destructive interference, the proposed pulse design can not recover the excitation because the pulse profile needs to have an infinity value.

This approach can be applied to a wide variety of applications. Kim et al. (19) demonstrated that nonuniform saturation due to B_1^+ inhomogeneity leads to regional contrast variations in first-pass myocardial perfusion imaging and suggested adiabatic composite (BIR-4) pulses (20) as a solution. BIR-4 pulses work well but their use is limited by SAR, especially at 3T or higher field strength. Similar to the proposed 2DRF pulse, tailored 1D saturation pulses can be designed to saturate uniformly over LV with a much lower RF power. This may be useful in the applications where SAR is a critical constraint such as first-pass perfusion imaging with more than 5 slices per heart-beat.

The proposed method is based on unidirectional B_1^+ variation, which may apply to other body areas, especially when focusing on an ROI. Figure 8 contains an example of ROI-based B_1^+ compensation in head imaging at 3T. An axial

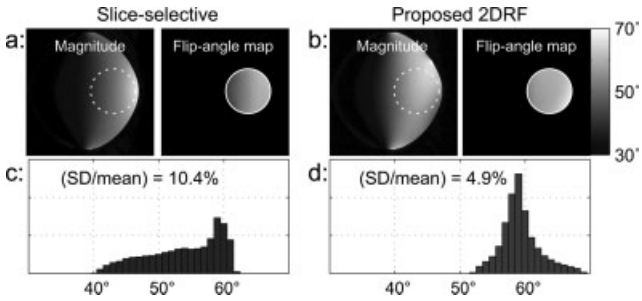

FIG. 5. Phantom Validation. The flip angle varied from left (low flip angle) to right (high flip angle) using a conventional slice-selective RF pulse. The proposed 2DRF was used to correct unidirectional flip angle variation over the ROI (white dotted circle). Magnitude images and flip angle distributions are shown (**a** and **b**) along with the corresponding flip angle histograms (**c** and **d**). The flip angle SD/mean within the ROI was improved from 10.4% (53.9° ± 5.6°) to 4.9% (59.3° ± 2.9°) using the proposed 2DRF approach.

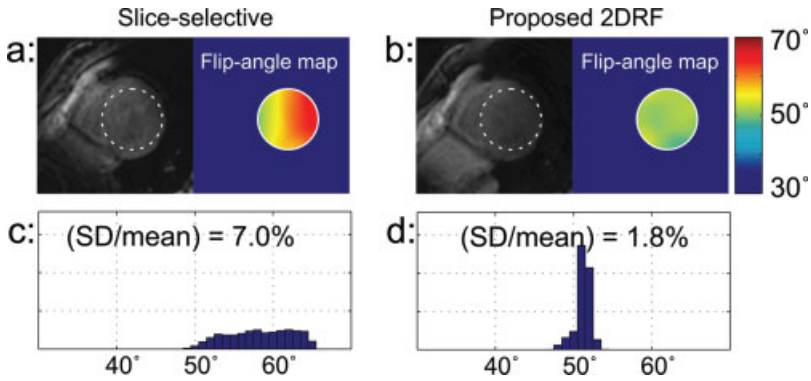

FIG. 6. Cardiac B_1^+ inhomogeneity compensation in a healthy volunteer at 3T. Magnitude images and flip angle distributions are shown (**a** and **b**) along with the corresponding flip angle histograms (**c** and **d**). Magnitude images are shown for anatomical landmarks. The value of SD/mean within the left ventricle (white circle) was improved from 7.0% (58.3° ± 4.1°) to 1.8% (51.2° ± 0.9°) using the proposed 2DRF pulse.

scan plane was prescribed and two symmetric ROIs containing white matter were manually selected. For ROI A, the value of SD/mean was reduced from 6.5% (55° ± 3.6°) to 1.9% (62° ± 1.2°) using the proposed 2DRF approach. For ROI B, the value of SD/mean was reduced from 7.1% (55° ± 3.9°) to 1.9% (59° ± 1.1°) using the proposed 2DRF approach.

Off-resonance during 2DRF fly-back echo-planar excitation creates a linear phase along k_r, and results in a shift in $\widehat{f}(r)$ along the r-axis (see Fig. 3). This can be modeled as spatially varying phase increment $\Delta\theta(x,y)$ in addition to θ. $\Delta\theta(x,y)$ can have a range of ±46.8° based on the typical off-resonance range (±130 Hz) over the LV at 3T (21). Although not problematic in our studies, this may be an issue when using longer subpulses. Localized center frequency and ROI-based shimming are highly desirable in this case (22). High-order shimming would decrease the off-resonance range to ±90 Hz over the LV at 3T (21), and may be helpful in improving the accuracy of B_1^+ compensation.

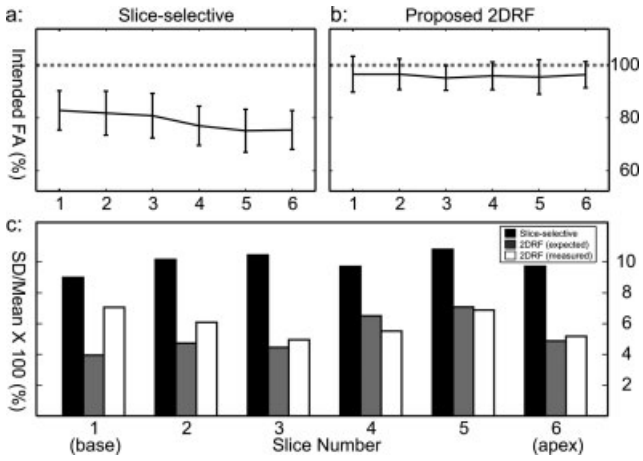

FIG. 7. Whole heart B_1^+ inhomogeneity compensation in a healthy volunteer at 3T. Mean and SD plots (**a** and **b**) are compared for conventional excitation and the proposed compensating 2DRF excitation for six short-axis slices. The gray dotted line indicates the intended flip angle (100%). The SD/mean values (**c**) were computed for slice-selective and 2DRF (expected in simulation and measured). Note that the expected (gray bars) and measured (white bars) values show an excellent agreement except in the basal slice.

The calculation of the control parameters is based on a B_1^+ profile that is measured in a separate breath-hold. Respiratory motion may create differences in slice position. This small image mis-registration may not affect the overall quality due to the low spatial resolution (5 mm), unless B_1^+ patterns vary with breath-hold position. The investigation of the intrinsic B_1^+ variation between exhale and inhale positions would be helpful to understand how much this may or may not influence the performance of measurement-based B_1^+ compensation.

Our initial RF pulse design confined the number of subpulses to three and used a 1-2-1 subpulse weighting for simplicity and to minimize pulse duration. The number of subpulses could be increased, and the subpulse weightings could be free parameters to add more degrees of freedom

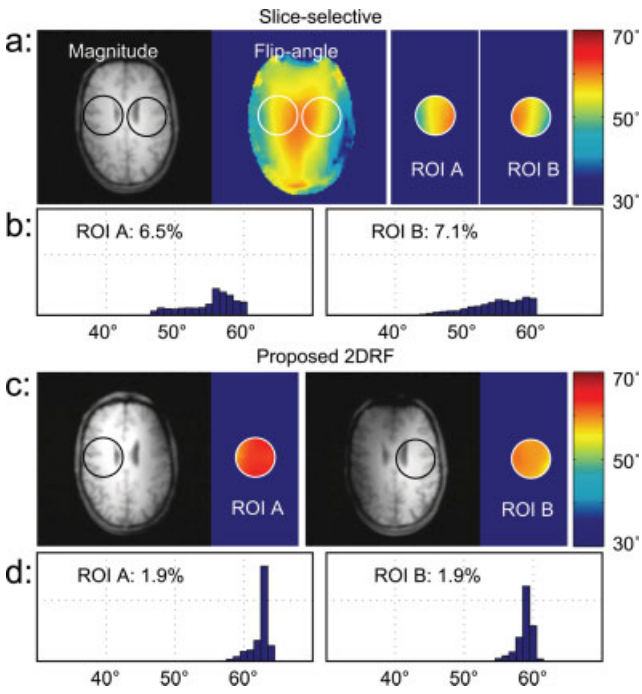

FIG. 8. ROI-based B_1^+ inhomogeneity compensation in the head of a healthy volunteer at 3T. The B_1^+ profile was parabolic in shape and two symmetric ROIs (A and B) were selected. Using the proposed 2DRF approach, the flip angle SD/mean was improved from 6.5% to 1.9% when focusing on ROI A, and from 7.1% to 1.9% when focusing on ROI B.

to the in-plane profile variation $\widehat{f}(r)$, and potentially yield more accurate compensation. Any portion of the spectral response of the subpulse weights (conceptually and FIR filter) can be used to find the optimal profile. As such, the subpulse weights would then become additional control parameters.

The original design for the proposed 2DRF pulse (shown in Fig. 1) has duration of 3 msec and can accommodate a maximum flip angle of 60°. Although we redesigned the RF pulse (6 msec) to support a maximum flip angle of 180° for validation (used in Fig. 5–7), the original design is more useful in practice. The 3 msec pulse (used in Fig. 3–4) can compensate up to the intended flip angle of 40°. In addition, the original design has shorter RF subpulse duration (0.5 msec), and therefore the 3 msec pulse will be more resilient to off-resonance artifacts than the 6 msec pulse.

CONCLUSION

Short tailored 2DRF excitation pulses can be used to substantially reduce flip angle variation in cardiac imaging at 3T. The proposed RF pulse design can be dynamically adapted to different ROIs and patterns of B_1^+ variation by adjusting a few control parameters (primary in-plane axis, $\alpha_{\max}$, θ, and Δk_r). The proposed 2DRF pulse reduced the value of SD/mean over the LV by nearly a factor of two compared to conventional slice-selective RF excitation, in cardiac imaging at 3T. This type of reduction in flip angle variation is particularly important in high field imaging and quantitative imaging.

ACKNOWLEDGEMENTS

The authors thank Dr. Charles H. Cunningham for useful discussions and providing the pulse sequence for excitation profile measurement and Barry Vanek for helpful discussions during preparation of the manuscript.

REFERENCES

1. Greenman RL, Shirosky JE, Mulkern RV, Rofsky NM. Double inversion black-blood fast spin-echo imaging of the human heart: A comparison between 1.5T and 3.0T. J Magn Reson Imaging 2003;17:648–655.
2. Nayak KS, Cunningham CH, Santos JM, Pauly JM. Real-time cardiac MRI at 3 Tesla. Magn Reson Med 2004;51:655–660.
3. Vaughan J, Adriany G, Snyder C, Tian J, Thiel T, Bolinger L, Liu H, DelaBarre L, Ugurbil K. Efficient high-frequency body coil for high-field MRI. Magn Reson Med 2004;52:851–859.
4. Garwood M, Ke Y. Symmetric pulses to induce arbitrary flip angles with compensation for RF inhomogeneity and resonance offsets. J Magn Reson 1991;94:511–525.
5. Deichmann R. Optimized RF excitation for anatomical brain imaging of the occipital lobe using the 3D MDEFT sequence and a surface transmit coil. Magn Reson Med 2005;53:1212–1216.
6. Wen H, Denison TJ, Singerman RW, Balaban RS. The intrinsic signal-to-noise ratio in human cardiac imaging at 1.5, 3, and 4 T. J Magn Reson 1997;125:65–71.
7. Singerman RW, Denison TJ, Wen H, Balaban RS. Simulation of B_1 field distribution and intrinsic signal-to-noise in cardiac MRI as a function of static magnetic field. J Magn Reson 1997;125:72–83.
8. Cunningham CH, Pauly JM, Nayak KS. SDAM: Saturated double angle method for rapid B1+ mapping. Magn Reson Med 2006;55:1326–1333.
9. Sung K, Nayak KS. RF non-uniformity over the whole heart at 3T. In: Proceedings of ISMRM, 15th Annual Meeting, Berlin, 2007. p 355.
10. Deichmann R, Good CD, Turner R. RF inhomogeneity compensation in structural brain imaging. Magn Reson Med 2002;47:398–402.
11. Saekho S, Boada FE, Noll DC, Stenger VA. Small tip angle three-dimensional tailored radiofrequency slab-select pulse for reduced B1 inhomogeneity at 3 T. Magn Reson Med 2005;53:479–484.
12. Pauly JM, Nishimura DG, Macovski A. A k-space analysis of small tip excitation. J Magn Reson 1989;31:43–56.
13. Oelhafen M, Pruessmann KP, Kozerke S, Boesiger P. Calibration of echo-planar 2D-selective RF excitation pulses. Magn Reson Med 2004;52:1136–1145.
14. Bernstein MA, King KF, Zhou XJ. Handbook of MRI pulse sequences. New York: Academic Press; 2004.
15. Fredrickson JO, Meyer CH, Pelc NJ. Flow effects of spectral spatial excitation. In: Proceedings of ISMRM, 5th Annual Meeting, Vancouver, 1997. p 113.
16. Pauly JM, Roux PL, Nishimura DG, Macovski A. Parameter relations for the Shinnar-Le Roux selective excitation pulse design algorithm. IEEE Trans Med Imaging 1991;10:53–65.
17. Conolly S, Nishimura DG, Macovski A, Glover G. Variable-rate selective excitation. J Magn Reson 1988;78:440–458.
18. Stollberger R, Wach P. Imaging of the active B_1 field *in vivo*. Magn Reson Med 1996;35:246–251.
19. Kim D, Cernicanu A, Axel L. BO and B1-insensitive uniform T1-weighting for quantitative, first-pass myocardial perfusion magnetic resonance imaging. Magn Reson Med 2005;54:1423–1429.
20. Staewen RS, Johnson AJ, Ross BD, Parrish T, Merkle H, Garwood M. 3-D FLASH imaging using a single surface coil and a new adiabatic pulse, BIR-4. Invest Radiol 1990;25:559–567.
21. Noeske R, Seifert F, Rhein KH, Rinneberg H. Human cardiac imaging at 3 T using phased array coils. Magn Reson Med 2000;44:978–982.
22. Schar M, Kozerke S, Fischer SE, Boesiger P. Cardiac SSFP imaging at 3 Tesla. Magn Reson Med 2004;51:799–806.